RECENZIRANI ČLANKI | PEER-REVIEWED ARTICLES

Vrednotenje delovanja cenovno ugodnega sprejemnika GNSS z uporabo različnih geodetskih anten v okviru ničelnega baznega vektorja

Performance Evaluation of Low-Cost GNSS Receiver Using Different Geodetic Antennas in a Zero Baseline Configuration

Rosendo Romero-Andrade, Norberto Alcantar-Elizondo, Tiojari D. Guzmán-Galindo, Jorge A. Cañedo -Pérez, Yedid Gpe. Zambrano-Medina, Rafaela M. Llanes-Hernández

UDK: 528.23:629.056.8
Klasifikacija prispevka po COBISS.SI: 1.01
Prispelo: 11. 3. 2026
Sprejeto: 21. 5. 2026

DOI: 10.15292/geodetski-vestnik.2026.03.406-420
SCIENTIFIC ARTICLE
Received: 11. 3. 2026
Accepted: 21. 5. 2026

SI | EN

IZVLEČEK

Zmogljivost cenovno ugodnega sprejemnika GNSS (ZED F9P) je ocenjena z uporabo konfiguracije ničelnega baznega vektorja in primerjana s sprejemnikom geodetske kakovosti z uporabo različnih modelov anten geodetske in nizkocenovne kakovosti ter različnih kombinacij GNSS-konstelacij. Študija se osredotoča na analizo koordinat ENU, pristranskosti in skupnega standardnega odklona, pri čemer upošteva tako konfiguracije z eno samo konstelacijo kot konfiguracije z več konstelacijami. Rezultati kažejo, da lahko cenovno ugodni GNSS-sprejemniki dosežejo natančnost in točnost, primerljivo z geodetskimi instrumenti, samo z uporabo ustrezno kalibriranih anten. Kombinacija GPS+GALILEO izboljša zmogljivost le, če se uporabljajo kalibrirane antene, medtem ko konstelacije GLONASS in GALILEO, obdelane neodvisno ali v kombinaciji, kažejo precejšnje omejitve pri uporabi cenovno ugodnih sprejemnikov, kar preprečuje doseganje robustnih rešitev v obravnavanih pogojih. Rezultati kažejo, da so cenovno ugodni GNSS-sprejemniki lahko alternativa za topografsko-geodetske naloge, če je konstelacija GPS na voljo in če to omogočajo projektne zahteve in pogoji opazovanja. Poleg tega je dokazano, da vključitev več konstelacij sama po sebi ne zagotavlja izboljšanja natančnosti pozicioniranja pri uporabi cenovno ugodnih sprejemnikov.

ABSTRACT

The performance of a low-cost GNSS receiver (ZED F9P) is evaluated using a zero-baseline configuration and compared with a geodetic-grade receiver through the use of different geodetic-grade and low-cost antenna models, as well as different GNSS constellation combinations. The study focuses on the analysis of ENU coordinates, bias, and total standard deviation, considering both single-constellation and multi-constellation configurations. The results demonstrate that low-cost GNSS receivers can achieve precision and accuracy comparable to those of geodetic-grade equipment when appropriately calibrated antennas are used. The GPS+GALILEO combination improves performance only when calibrated antennas are used, whereas the GLONASS and GALILEO constellations, processed independently or in combination, exhibit significant limitations when applied to low-cost receivers, preventing the attainment of robust solutions under the evaluated conditions. The results indicate that low-cost GNSS receivers constitute a viable alternative for topographic–geodetic applications, provided that the GPS constellation is available and that the project requirements and observation conditions allow it. Furthermore, it is shown that the inclusion of multiple constellations does not, by itself, guarantee an improvement in positioning precision when low-cost receivers are used.

KLJUČNE BESEDE

GNSS, cenovno ugodno sprejemniki, konfiguracija ničelnega baznega vektorja, geodetske in cenovno ugodne antene

KEY WORDS

GNSS, low-cost GNSS receiver, zero-baseline configuration, geodetic-grade and low-cost antennas

1 introduction

With the advancement of technology, and particularly with the development of Global Navigation Satellite Systems (GNSS), new electronic devices have emerged, including low-cost receivers capable of tracking the different constellations that comprise GNSS in a manner comparable to geodetic-grade receivers. The term "low-cost" is adopted due to their average price of approximately 5,000 MNX, in contrast to geodetic-grade receivers, which can cost no less than 80,000 MNX. These low-cost receivers are highly sensitive, as they feature signal tracking capabilities reaching an average of –160 dBm, compared to geodetic receivers, which typically reach an average of –128.5 dBm (Tsakiri et al., 2017; Zamora-Maciel et al., 2020). Nevertheless, their positioning accuracy ultimately depends on the processing models employed (Ferhat et al., 2015).

In this sense, geodetic receivers were initially used for mapping purposes (Sioulis et al., 2015), as they did not provide high precision due to being single-frequency devices. Over time, low-cost equipment has been tested in different environments, with the Precise Point Positioning (PPP) technique (Romero-Andrade et al., 2019) being one of the most extensively studied, as it does not require a reference station to determine precise coordinates. Likewise, low-cost receivers have been tested for monitoring dam displacements (Romero-Andrade et al. 2024), total electron content analysis (Bagheri & Dabove, 2025), and deformation monitoring oriented toward Structural Health Monitoring (SHM) (Chen et al., 2024), among other applications.

Tunini et al. (2022) demonstrated that millimeter-level accuracy can be achieved by analyzing long time series, comparable to those obtained with geodetic-grade equipment. For topographic and geodetic applications, low-cost receivers have also been tested in different (Bojorquez-Pacheco et al., 2022, 2023; Romero-Andrade et al., 2020; Santiago-Sánchez et al., 2024), highlighting the high precision that can be achieved when geodetic-grade antennas are combined with low-cost receivers. However, these studies were limited to the use of the GPS system only.

Zuliani et al. (2022) developed a multipurpose GNSS-based platform, demonstrating that single- and dual-frequency receivers can be used for cadastral, monitoring, educational, and professional applications, achieving centimeter- to millimeter-level accuracy depending on the processing strategy applied. Nevertheless, the type of antenna plays a crucial role. In this regard, , Krietemeyer et al. (2022) developed software to establish the calibration of low-cost antennas (since they are not calibrated by official agencies), showing that low-cost antennas can also be used for crustal deformation applications, achieving millimeter-level precision.

Hamza et al. (2023) used dual-frequency low-cost GNSS receivers for continuous monitoring of landslides, installing four stations with a six-month observation period. The observations were processed in relative static mode, achieving differences of less than 7 mm compared to geodetic equipment. However, it was also shown that small displacements were not reliably detected in the vertical component.

Regarding positioning time, Kazmierski et al. (2023) evaluated positioning quality using low-cost GNSS receivers in both long (24 h) and short (10 min) sessions, demonstrating millimeter-level repeatability over a precise baseline. The low-cost receivers achieved maximum errors of 17 mm horizontally and 40 mm in height.

Furthermore, Hernández-Andrade, Daniel et al. (2024) analyzed a geodetic baseline using low-cost receivers, geodetic-grade equipment, and direct measurements obtained with an electronic total station. Through statistical testing, they demonstrated that low-cost receivers are viable for geodetic applications, as the observed variations were statistically comparable.

Although low-cost equipment has been analyzed from multiple perspectives, Stopar et al. (2024) conducted a state-of-the-art review of low-cost receivers, showing that precision comparable to geodetic-grade equipment can be achieved. However, they did not analyze multi-constellation GNSS performance, as not all receivers are capable of tracking all constellations. Similarly, they emphasized that the antenna environment is critical, as it directly affects positioning accuracy. Finally, Yang et al. (2025), presented a novel application analyzing total electron content as a seismic precursor, demonstrating that while the precision is lower than that of geodetic-grade receivers, the results are consistent. Table 1 summarizes representative studies related to low-cost GNSS receivers, highlighting the receiver type, antenna configuration, processing strategy, constellation combinations, and the main contribution of each study in comparison with the present work.

Table 1: Summary of representative studies related to low-cost GNSS positioning and comparison with the present study.

Study	Receiver Type	Antenna Type	Processing Strategy	Observation Configuration	Constellations	Main Contribution
Romero-Andrade et al. (2019)	Low-cost GNSS	Low-cost	PPP	Static	GPS	Comparative PPP analysis using low-cost GNSS receivers
Tunini et al. (2022)	Low-cost GNSS	Low-cost	Static processing	Long time series	GPS/GNSS	Millimeter-level crustal deformation monitoring
Krietemeyer et al. (2022)	Low-cost dual-frequency	Low-cost calibrated antennas	Relative/PPP	Field calibration	GPS/GLO/GAL	Calibration methodology for low-cost antennas
Zuliani et al. (2022)	Low-cost GNSS platform	Multiple antenna types	Relative/PPP	Static and kinematic	Multi-constellation	Multipurpose low-cost GNSS applications
Hamza et al. (2021)	Multi-frequency low-cost GNSS	Low-cost and geodetic-grade	Relative static	Zero-baseline	GPS/GLO/GAL	Evaluation of receiver and antenna performance
Hamza et al. (2023)	Low-cost dual-frequency GNSS	Geodetic-grade	Relative static	Continuous monitoring	GPS/GNSS	Landslide monitoring using low-cost GNSS
Bojorquez-Pacheco et al. (2023)	ZED-F9P	Geodetic-grade antennas	Relative static	Baseline	GPS	Static positioning evaluation of low-cost GNSS
Stopar et al. (2024)	Multiple low-cost GNSS receivers	Multiple	Review	Multiple	Multi-constellation	Review of observation and positioning quality of low-cost GNSS receivers
Konakoglu & Yilmaz, (2024)	Geodetic-grade GNSS	Geodetic-grade	PPP-AR	Forest environment	GPS/GPS + GLONASS	Influence of environment and constellation selection on PPP-AR

Study	Receiver Type	Antenna Type	Processing Strategy	Observation Configuration	Constellations	Main Contribution
This study	ZED-F9P and geodetic-grade receiver	Calibrated and non-calibrated antennas	PPP	Controlled zero-baseline	GPS, GLONASS, GALILEO and combinations	Joint evaluation of receiver type, antenna calibration status, and constellation combinations under controlled PPP conditions

Although previous studies have demonstrated that low-cost GNSS receivers can achieve high positioning precision under favorable conditions, most investigations have focused primarily on GPS-based solutions, individual antenna evaluations, or specific processing strategies. The combined influence of antenna calibration status, receiver type, and individual GNSS constellation configurations under controlled zero-baseline PPP conditions remains insufficiently discussed, particularly for GLONASS and GALILEO-based solutions using low-cost equipment. Furthermore, the inclusion of additional constellations does not necessarily guarantee improvements in positioning quality, especially when low-cost receivers and non-calibrated antennas are used.

Based on the above, it is evident that observation time and the inclusion of additional constellations remain key factors influencing the precision achieved. Therefore, the main objective of this study is to jointly evaluate the influence of receiver type, antenna model/calibration status, and different GNSS constellation combinations on PPP positioning performance using a controlled zero-baseline configuration. Special attention is given to the behavior of GLONASS and GALILEO-based solutions in comparison with GPS-based configurations using both geodetic-grade and low-cost antennas.

2 Methodology

2.1 General characteristics of the receivers and antennas used in the experiment

A geodetic-grade receiver (Figure 1A) and a low-cost receiver (Figure 1B) were used. As main characteristics, both devices have multi-constellation tracking capability and operate in dual frequency, configurable for both low and high frequencies. In this regard, the low-cost receiver used was the ZED-F9P model from u-blox, which presents a cold start period of 24 s, a reaction time of 2 s, and an average sensitivity of −167 dBm, according to the manufacturer. On the other hand, the geodetic-grade receiver employed was the SPS855 model from Trimble.

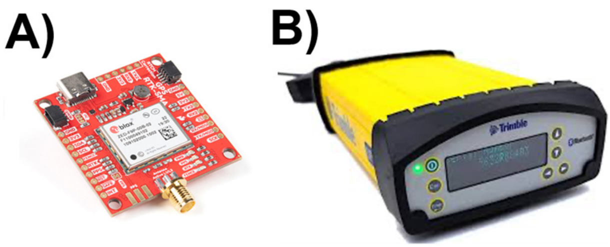

Figure 1: (A) Low-cost GNSS receiver, ZED-F9P model; (B) geodetic-grade receiver, SPS855 model from Trimble.

The geodetic-grade receiver and the low-cost receiver were connected through a certified signal splitter (Figure 2), which allows a single antenna to be connected and distributes the same signal to two receivers.

Figure 2: GNSS signal splitter.

As a complement to the observations, geodetic-grade antennas LEIAS10, ASH701975.01B, TRM11500, and LEIAT502 were used (Figure 3A–D), as well as two low-cost antennas, models BEIBT300 and AN600 (Figure 3E–F), the latter without calibration by the IGS.

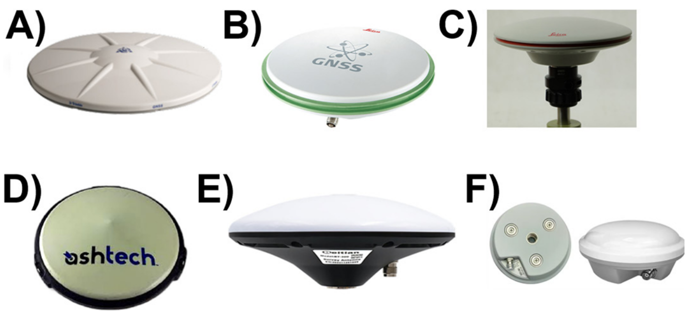

Figure 3: Antennas used in the study. (A) TRM11500; (B) LEIAS10; (C) LEIAT502; (D) ASH701975.01B; (E) BEIBT300; and (F) AN600.

In this regard, due to the different tracking capabilities of the antennas and receivers, only the GLONASS, GALILEO, and GPS constellations were considered. Table 2 summarizes the main characteristics of the antennas used in this study, including antenna type, calibration status, IGS nomenclature, ANTEX availability, and radome information.

Table 2: Characteristics of the antennas used in the experiment.

Antenna Model	Antenna Type	Calibration Status	IGS Antenna Code	ANTEX Available	Radome Information
TRM115000.10	Geodetic-grade	Calibrated	TRM115000.10	Yes	None
LEIAS10	Geodetic-grade	Calibrated	LEIAS10	Yes	None
LEIAT502	Geodetic-grade	Calibrated	LEIAT502	Yes	None
ASH701975.01B	Geodetic-grade	Calibrated	ASH701975.01B	Yes	None
BEIBT300	Low-cost	Calibrated	BEIBT300	Yes	None
AN600	Low-cost	Non-calibrated	Not available	No	None

2.2 GNSS Observation Collection, Pre-processing, and Processing

GNSS observations were carried out on March 28, 2025, under open-sky conditions, from 08:00 to 15:00 local time, with approximately one hour of continuous observation for each antenna configuration. All observations were performed sequentially at the same site using a zero-baseline configuration. The antennas were installed on a forced-centering geodetic pillar in order to minimize setup inconsistencies and guarantee repeatable antenna positioning during the observation sessions. Observations were recorded at a sampling interval of 1 Hz, due to the instability of the internal clock of the low-cost receiver (Romero-Andrade et al. 2021), and using an elevation angle of 15°, commonly considered between 10° and 15° to avoid signal obstructions (Hofmann-Wellenhof et al., 2008).

The experiment was conducted on a geodetic pillar located on the rooftop of the Faculty of Earth and Space Sciences building. The forced-centering pillar has an approximate height of 1.50 m and was installed under open-sky conditions with minimal nearby obstructions. These conditions allowed the evaluation of the intrinsic performance of the receiver–antenna configurations under controlled observation conditions while minimizing multipath effects. All observation sessions were conducted consecutively during stable weather conditions under clear-sky conditions and without significant geomagnetic disturbances reported during the observation period. Since all antenna configurations were evaluated at the same site and under similar environmental conditions, temporal variations associated with multipath and atmospheric effects were minimized.

The native files from the low-cost receivers in UBX format were converted to "obs" format using RTKLIB 2.4.5 b34 (Takasu, 2013). Similarly, the files from the geodetic-grade receiver were converted to RINEX format (Gurtner, 1994). In both cases, the observation files were edited and verified using RINGO software version 0.9.4 (Kawamoto et al., 2023), to check the consistency of parameters such as antenna height, antenna nomenclature according to the IGS standard, observation interval, and the observables recorded in the RINEX file. Antenna metadata, including antenna nomenclature, antenna height, and antenna reference point (ARP) consistency, were verified during the RINEX pre-processing stage according to IGS standards. For antennas with official IGS calibration models, the corresponding IGS nomenclature and ARP definitions were used. In the case of the AN600 antenna, no official IGS calibration or standardized antenna designation is currently available. Antenna heights were measured vertically from the top surface of the forced-centering pillar to the antenna reference mark indicated by the manufacturer, subtracting the screw height in order to maintain consistency between antenna configurations. In addition, all observations were conducted using a certified GNSS splitter, ensuring identical observation geometry for both receivers and minimizing receiver-dependent effects.

The observation files were processed using the Precise Point Positioning (PPP) technique (Hofmann-Wellenhof et al. 2008) with the PRIDE-PPPAR software (Linux version 3.2.4) (Geng et al., 2022), operating in static mode with ambiguity resolution enabled. Independent processing was performed for GPS (G12), GLONASS (R12), GALILEO (E15), and their combinations. Navigation and precise ephemeris products from the Wuhan analysis center were used together with the GPT3 tropospheric model and the VMF3 mapping function. The coordinates were referenced to ITRF2014, incorporating antenna corrections from the IGS20_2356 ANTEX model whenever available. Observation consistency and metadata verification were checked during the RINEX pre-processing stage using RINGO software, while strict observation editing was applied during PPP processing.

Reference coordinates used for the ENU transformation were obtained from a previous high-precision GNSS survey carried out with a Geomax Zenith25 geodetic-grade receiver. These coordinates were used as the control solution for evaluating each receiver–antenna–constellation configuration under the same reference framework. Therefore, the reported ENU differences and bias values represent relative deviations with respect to this control solution.

To analyze the GNSS solutions obtained, the coordinates were converted to North, East, and Up (ENU) coordinates with respect to the previously defined control solution. The analysis was performed independently for each constellation combination (GPS, GLONASS, GALILEO, GPS+GLONASS, GPS+GALILEO, GALILEO+GLONASS), considering the low-cost antenna and receiver, as well as the geodetic-grade receiver connected through a GNSS signal splitter, which guarantees that the observations were obtained under the same conditions.

In this sense, to analyze the bias generated between the obtained coordinates and the reference coordinates, the three-dimensional magnitude of the error was calculated for each station from the ENU coordinates (Equation 1):

$$BIAS = \sqrt{E^2 + N^2 + U^2} \tag{1}$$

Where E, N, and U represent the differences in the topocentric coordinates. Similarly, the total dispersion of the solutions was estimated from the standard deviations (Equation 2) of the geodetic coordinates using the following equation:

$$STD_{total} = \sqrt{\sigma_\varphi^2 + \sigma_\lambda^2 + \sigma_h^2} \tag{2}$$

Where σ_φ^2 represents the standard deviation of the geodetic latitude, σ_λ^2 represents the standard deviation of the geodetic longitude, and σ_h^2 represents the standard deviation of the ellipsoidal height. The parameter STD_{total} represents a global measure of precision.

In this study, positioning accuracy is interpreted from the ENU coordinate differences and three-dimensional bias values with respect to the reference solution, whereas positioning precision is evaluated through the component-wise and total standard deviations of the obtained solutions.

3 Results

A complete quantitative summary of the positioning performance obtained for all receiver–antenna–constellation configurations is provided in Appendix A (Table A1), including ENU coordinate differences, three-dimensional bias, standard deviations, and satellite availability. Figure 4 presents the results of the differences obtained from the GPS (G) + GALILEO (E) + GLONASS (R) combination for each antenna, as well as the biases and standard deviations (Figure 5). The largest difference is observed for the ASH701975.01B antenna when used with the geodetic-grade receiver, reaching a value of 0.0914 m. However, this same antenna shows the smallest difference when used with the low-cost receiver, with a value of 0.007 m. This behavior is technically interesting, since larger discrepancies were obtained with the geodetic-grade receiver, whereas smaller differences were observed with the low-cost receiver. Although the exact cause was not specifically evaluated in this study, the observed behavior may be associated with factors such as vertical-component sensitivity, antenna phasecenter correction modeling, ANTEX matching, satellite geometry during the observation session, or constellation-dependent processing effects. Therefore, additional controlled experiments are required to further investigate this behavior and confirm its reproducibility. In this case, the discrepancy associated with the geodetic-grade receiver appears to be strongly influenced by the vertical component, which presents the largest difference.

Regarding the smallest differences obtained with the geodetic-grade receiver, the non-calibrated low-cost antenna AN600 achieved a value of 0.014 m, showing consistent behavior by also presenting a reduced difference of 0.016 m when used together with the low-cost receiver. On the other hand, when considering exclusively the performance with the low-cost receiver, the ASH701975.01B antenna exhibits the smallest difference, with a value of 0.007 m.

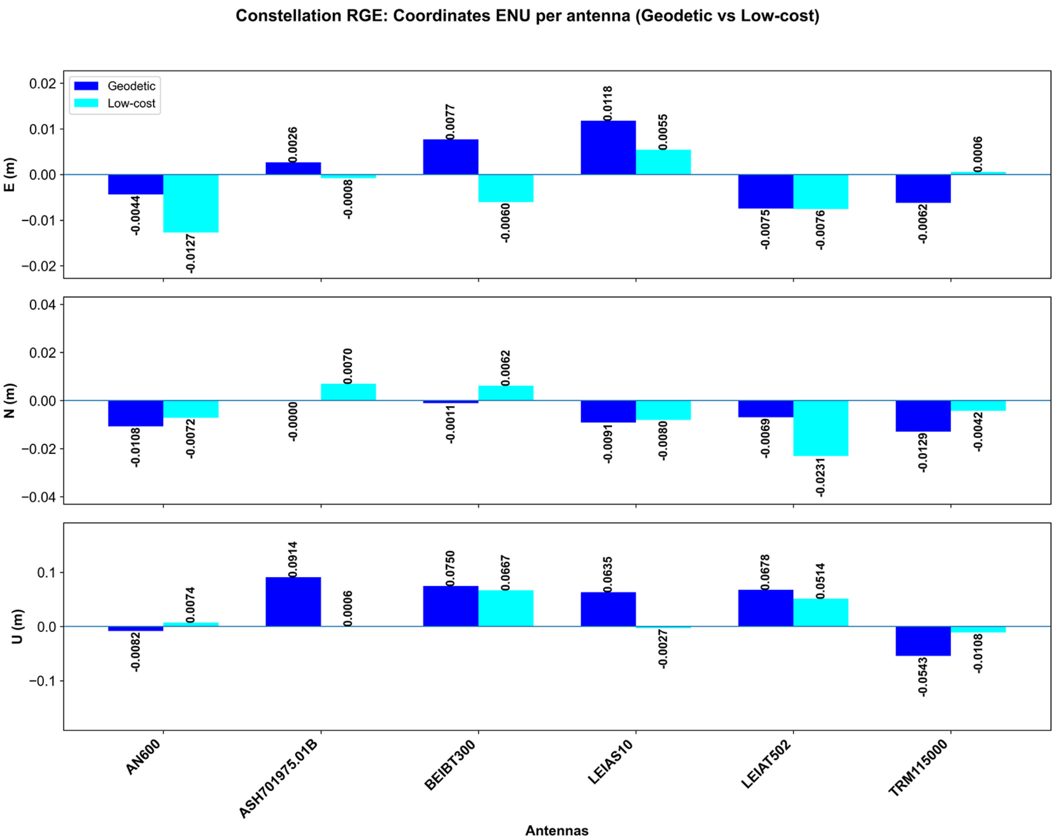

Figure 4: ENU coordinates for the geodetic-grade and low-cost receivers using different antennas with the GLONASS + GALILEO + GPS constellations.

With respect to the bias, it can be observed that the vertical component contributes negatively to the results; however, the overall dispersion remains at the millimeter level for most GPS-based configurations. According to the obtained results, in most antennas the geodetic-grade receiver exhibits larger biases than the low-cost receiver, indicating that the bias is not controlled solely by the receiver type and may be influenced by the antenna–receiver combination and calibration.

In this sense, the non-calibrated low-cost antenna AN600 presents results ranging from ≈0.014–0.016 m, with standard deviations <0.001 m, showing stable behavior for both receivers. In contrast, the geodetic-grade antenna ASH701975.01B presents the largest bias when used with the geodetic receiver, reaching a value of 0.091 m, while it also achieves the smallest bias when used with the low-cost receiver, with a value of 0.007 m.

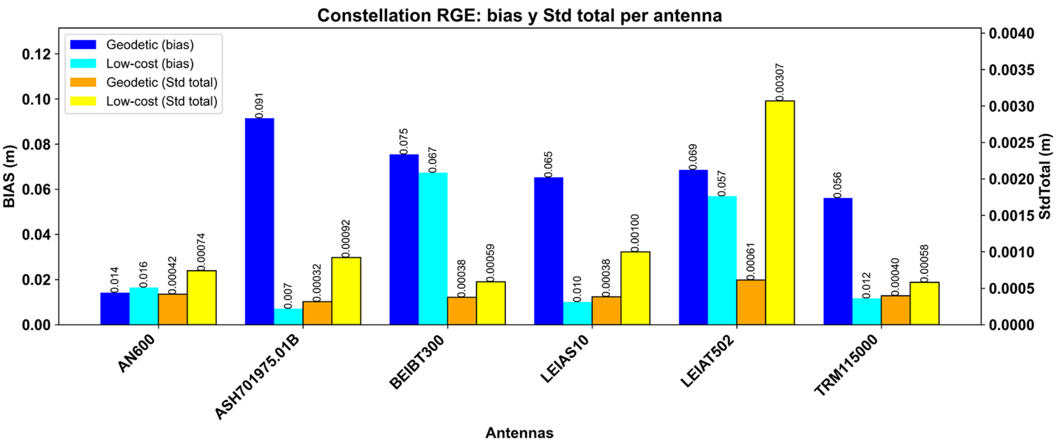

Figure 5: Bias and total standard deviation by antenna and receiver type using the GLONASS + GALILEO + GPS constellations.

Figure 6 presents the differences corresponding to the GLONASS + GPS combination for both the geodetic-grade receiver and the low-cost receiver. In both cases, the horizontal components remain at the millimeter level, while the vertical component reaches centimeter-level values. However, for the LEIAS10 geodetic antenna and the uncalibrated AN600 antenna, the observed differences in all components remain at the millimeter level, regardless of the type of receiver used.

Regarding the bias (Figure 7), it is observed that for most antenna–receiver combinations, the values fall within the centimeter range. The only exception corresponds to the ASH701975.01B antenna combined with the low-cost receiver, which exhibits both bias and total standard deviation at the millimeter level, showing a notably more stable behavior compared to the rest of the analyzed configurations.

For the ENU coordinates of the GPS + GALILEO combination (Figure 8), it is observed that geodetic-grade receivers using geodetic antennas present the smallest differences. However, the case of the TRM115000 antenna stands out, showing centimeter-level differences in the North and Vertical components. Similarly, the LEIAS10 antenna exhibits comparable behavior, although with millimeter-level differences. Likewise, for the low-cost receiver, the smallest difference is obtained when using the ASH701975.01B geodetic antenna, whereas the uncalibrated AN600 antenna presents the largest differences, reaching centimeter-level values.

Figure 9 presents the bias and total standard deviation for the GPS + GALILEO combination. The configuration formed by the low-cost receiver and the uncalibrated AN600 antenna shows the worst performance, reaching biases exceeding 20 cm and a significant degradation in precision. In contrast, the rest of the combinations, both with geodetic-grade and low-cost receivers, present biases within the centimeter range or smaller. Most configurations exhibit millimeter-level values, with the low-cost receiver combined with the AN600 antenna being the only case with significantly larger dispersion.

Figure 10 shows the ENU components for the GLONASS + GALILEO combination. While the solutions obtained with geodetic-grade receivers exhibit stable behavior, with millimeter- to centimeter-level displacements, the low-cost receivers display large differences in the three components, reaching meter-level errors, even when calibrated geodetic antennas are used. These results indicate that, for this constellation combination, the large differences observed with the low-cost receiver are not dominated by the antenna but rather by receiver limitations. The bias and total standard deviation shown in Figure 11 for the GLONASS + GALILEO combination confirms this behavior: solutions with geodetic-grade receivers present centimeter-level biases and millimeter precision, whereas low-cost receivers exhibit meter-level biases and standard deviations reaching meter-level values, even when calibrated geodetic antennas are used.

Figures 12 and 13 present the ENU components, bias, and total standard deviation for the GLONASS constellation. The results obtained with geodetic-grade receivers show stable behavior, with decimeter-level biases and millimeter precision for all evaluated antennas. In contrast, low-cost receivers present meter-level biases and standard deviations exceeding 10 m, even when calibrated geodetic antennas are used. The analysis of the ENU components reveals significant systematic displacements, particularly in the vertical component.

Figures 14 and 15 present the ENU components and the bias together with the total standard deviation for the GPS constellation, respectively. Unlike the previous combinations, both geodetic-grade and low-cost receivers show stable behavior, with centimeter-level biases and millimeter precision. The main degradation occurs when the uncalibrated AN600 antenna is used with the low-cost receiver, reaching biases close to 20 cm. For the rest of the antennas, the differences between both receiver types are negligible, confirming the robustness of the GPS constellation and highlighting the dominant role of antenna calibration in the quality of the solution.

Finally, Figures 16 and 17 present the ENU components, bias, and total standard deviation for the GALILEO constellation, respectively. The results obtained with geodetic-grade receivers show millimeter-level precision; however, centimeter- to decimeter-level biases are observed, mainly dominated by the vertical component, particularly for the BEIBT300 antenna, despite being a calibrated antenna.

Table 3 presents the number of satellites tracked per constellation for both low-cost and geodetic-grade equipment, as well as for each antenna. It can be observed that, for all observations, an average of 44 satellites in the visible sky was reached. Additionally, Figures 18 and 19 show the satellite tracking per hour, confirming that more than four satellites per constellation were always tracked.

Table 3: Number of satellites tracked per constellation, receiver, and antenna.

Receiver	Antenna	Constellation	Number of Satellites
Trimble SPS855	AN600 NONE	GPS	10
		GALILEO	6
		GLONASS	7
	LEIAS10 NONE	GPS	12
		GALILEO	10
		GLONASS	5

Receiver	Antenna	Constellation	Number of Satellites
Trimble SPS855	ASH701975.01B NONE	GPS	10
		GALILEO	11
		GLONASS	10
	LEIAT502 NONE	GPS	11
		GALILEO	0
		GLONASS	10
	BEIBT300 NONE	GPS	11
		GALILEO	5
		GLONASS	6
	TRM115000.10 NONE	GPS	10
		GALILEO	7
		GLONASS	6
ZED F9P	AN600	GPS	11
		GALILEO	9
		GLONASS	11
	LEIAS10	GPS	15
		GALILEO	14
		GLONASS	10
	ASH701975.01B	GPS	13
		GALILEO	11
		GLONASS	15
	LEIAT502	GPS	13
		GALILEO	12
		GLONASS	8
	BEIBT300	GPS	12
		GALILEO	12
		GLONASS	10
	TRM115000.10	GPS	14
		GALILEO	13
		GLONASS	11

4 Discussion

The results obtained demonstrate that low-cost GNSS equipment can achieve precision and accuracy comparable to those of geodetic-grade equipment, particularly when calibrated antennas are used, as reported by Krietemeyer et al. (2022) and corroborated by the experimentation carried out in this study. However, the type of constellation combination directly impacts the precision and accuracy, and consequently the type of application for which these configurations can be recommended. In any case, whenever the GPS constellation is present, low-cost equipment can be used for topographic–geodetic applications, provided that the project requirements allow it.

On the other hand, the GPS, GALILEO, and GLONASS constellations, when processed independently, show significant limitations in terms of the precision and accuracy achieved when low-cost receivers are used. Likewise, the GALILEO + GLONASS combination does not provide improvements in precision when using low-cost equipment, reaching meter-level errors. These results confirm that the use of low-cost receivers in topographic–geodetic applications depend on using the GPS constellation as the primary system, while other constellations may be incorporated as complementary systems whenever possible.

Although the independent GLONASS, GALILEO, and GLONASS+GALILEO-based solutions obtained with the low-cost receiver exhibited significantly larger errors, these results should be interpreted cautiously. The observed degradation may not depend exclusively on the receiver itself, but also on factors such as satellite geometry, observation duration, ambiguity convergence behavior, antenna calibration status, and constellation-dependent processing performance. Since detailed diagnostic indicators such as DOP values, residual analysis, and cycle-slip statistics were not evaluated in this study, additional experiments are required before attributing the observed behavior exclusively to receiver limitations.

In this sense, as is well known, the GPS constellation exhibits the most stable behavior; however, its performance improves when integrated with the GLONASS and GALILEO constellations, provided that site conditions and satellite geometry are favorable. The largest discrepancies are systematically observed in the vertical component, although the use of multi-constellation GNSS solutions contributes to a significant improvement in its precision. The obtained results also confirm that the vertical component remains the most sensitive parameter in PPP solutions, particularly when low-cost equipment or non-calibrated antennas are used. This behavior is consistent with the limitations of vertical positioning. In this sense, antenna calibration plays a fundamental role, since non-calibrated antennas may introduce systematic effects that become more evident in the vertical component, even when horizontal precision remains stable.

Previous studies, such as those conducted by Hamza et al. (2020), (2021), indicate that it is possible to achieve high precision using low-cost receivers, although this strongly depends on the type of antenna employed. Consistently, our results confirm that the combination of a low-cost receiver with a geodetic-grade antenna represents a viable alternative for obtaining high-precision solutions. Likewise, according to Romero-Andrade et al. (2021) it is possible to achieve high precision with low-cost receivers, although the results depend strongly on the antenna used. Our findings confirm that the combination of a low-cost receiver with a geodetic-grade antenna is a viable alternative for achieving high-precision solutions. Furthermore, as reported by Bojorquez-Pacheco et al. (2022), (2023); Santiago-Sánchez et al. (2024) millimeter-level differences can be achieved, comparable to those obtained in this study; however, these studies are limited exclusively to the use of the GPS constellation.

It is important to note that the present study was conducted under controlled short-session zero-baseline conditions using observations acquired during a single day with approximately one-hour sessions per antenna configuration. Therefore, the obtained results should be interpreted within the evaluated experimental framework, since PPP convergence behavior, satellite geometry, atmospheric conditions, and multipath effects may vary under longer observation periods and different environmental conditions. Consequently, additional experiments under diverse environments, repeated sessions, and longer observation durations are recommended in future work to further validate the observed behavior of low-cost GNSS receivers and antenna configurations.

5 Conclusions

This study presents the evaluation of different geodetic-grade antennas in combination with a low-cost GNSS receiver and a geodetic-grade receiver, both used in a zero-baseline configuration. The results obtained allow the following conclusions to be drawn:

Low-cost GNSS receivers, particularly the ZED-F9P model, can achieve precision and accuracy comparable to geodetic-grade receivers, provided that calibrated geodetic antennas are used. These results also depend on the processing applied to the observations.

The results confirm that performance is not determined solely by the type of receiver, but rather by the receiver–antenna–constellation configuration employed.

The GPS constellation, as widely recognized, is the most robust and stable, which is confirmed in this study. However, when combined with other constellations, the following situations are observed:

The GALILEO + GPS combination improves results only when calibrated antennas are used, whereas uncalibrated antennas introduce significant errors in low-cost receivers.

The GLONASS + GALILEO combination exhibited the largest positioning discrepancies under the evaluated experimental conditions, particularly when low-cost receivers and non-calibrated antennas were used.

The GLONASS and GALILEO constellations processed independently present limitations when used with low-cost receivers, making them unsuitable for topographic applications. In the case of geodetic-grade receivers, their use may still be possible depending on the project requirements.

Among the analyzed combinations, the vertical component remains the most challenging, as it is the least precise. Nevertheless, the inclusion of additional constellations alongside GPS improves the stability of the vertical component, although this improvement depends on the site conditions and the system configuration.

The results confirm that low-cost GNSS receivers can be used in topographic–geodetic applications, provided that the GPS constellation is included and that the project requirements (precision, environment, and processing strategy) allow it. However, the vertical component remains the most critical parameter to evaluate. Finally, this study demonstrates that the inclusion of additional constellations does not necessarily guarantee improvements in precision and accuracy, particularly for low-cost equipment. Under the evaluated short-session PPP conditions, GPS-based configurations exhibited the most stable and consistent behavior, whereas independent GLONASS- and GALILEO-based solutions presented larger positioning discrepancies when low-cost equipment was used.

Acknowledgements

The authors gratefully acknowledge the financial and academic support provided by the Secretaría de Ciencia, Humanidades, Tecnología e Innovación (SECIHTI), Mexico, through the National System of Researchers (SNII). The authors also thank the Universidad Autónoma de Sinaloa (UAS), particularly the Faculty of Earth and Space Sciences, for the institutional and logistical support that made this research possible.

Appendix is accessible at https://geodetski-vestnik.com/arhiv/70/3/Appendix_2

References

Bagheri, M., & Dabove, P. (2025). Navigating the Storm: Assessing the Impact of Geomagnetic Disturbances on Low-Cost GNSS Permanent Stations. Remote Sensing, 17(17), 2933. https://doi.org/10.3390/rs17172933

Bojorquez-Pacheco, N., Romero-Andrade, R., Trejo-soto, M. E., Hernádez-Andrade, D., & Trejo-Echeagaray, M. (2022). Evaluación del posicionamiento preciso a través de los receptores GPS LEA-6T , NEO-M8T y ZED-F9P de bajo costo. European Scientific Journal, 68–89. https://doi.org/10.19044/esj.2022.v18n24p68

Bojorquez-Pacheco, N., Romero-Andrade, R., Trejo-Soto, M. E., Hernández-Andrade, D., Nayak, K., Vidal-Vega, A. I., Arana-Medina, A. I., Sharma, G., Acosta-gonzález, L. E., & Serrano-Agila, R. (2023). Performance evaluation of single and double-frequency low-cost GNSS receivers in Static Relative mode. Geodetski Vestnik, 67(2), 244–257. https://doi.org/10.15292/geodetski-vestnik.2023.02.244-257

Chen, M., Zhao, L., Zhai, W., Lv, Y., & Jin, S. (2024). Assessment of the Real-Time and Rapid Precise Point Positioning Performance Using Geodetic and Low-Cost GNSS Receivers. Remote Sensing, 16(8). https://doi.org/10.3390/rs16081434

Ferhat, G., Malet, J.-P., & Ulrich, P. (2015). Evaluation of different processing strategies of Continuous GPS (CGPS) observations for landslide monitoring. EGU General Assembly Conference Abstracts, 17, 10582.

Geng, J., Ge, M., Yang, S., Zhang, K., Lin, J., Li, W., Mao, S., & Pan, Y. (2022). PRIDE PPP-AR II (II). GNSS Research Center, Wuhan University.

Gurtner, W. (1994). INNOVATION: RINEX--THE RECEIVER INDEPENDENT EXCHANGE FORMAT. GPS World, 5(7), 48–53.

Hamza, V., Stopar, B., & Ambrožic, T. (2020). Testing Multi-Frequency Low-Cost GNSS Receivers for Geodetic Monitoring Purposes. Sensors, 20, 16. https://doi.org/10.3390/s20164375

Hamza, V., Stopar, B., & Sterle, O. (2021). Testing the performance of multi-frequency low-cost GNSS receivers and antennas. Sensors, 21(6), 1–16. https://doi.org/10.3390/s21062029

Hamza, V., Stopar, B., Sterle, O., & Pavlovčič-Prešeren, P. (2023). A Cost-Effective GNSS Solution for Continuous Monitoring of Landslides. Remote Sensing, 15(9). https://doi.org/10.3390/rs15092287

Hernández-Andrade, Daniel, de Lacy-Pérez de los Cobos, M. C. P., Romero-Andrade, R., & Trejo-Soto, M. E. (2024). Statistical Comparison of Geodetic Baseline for Topographic – Geodetic Purposes Using a Low-Cost GNSS Receiver and Electromagnetic Distance Measurement. Journal of Surveying Engineering, 150(1), 1–10. https://doi.org/10.1061/JSUED2.SUENG-1446

Hofmann-Wellenhof, B., Lichtenegger, H., & Wasle, E. (2008). GNSS Global Navigation Satellite System GPS, GLONASS, Galileo and more. Springer Wien New York.

Kawamoto, S., Takamatsu, N., & Abe, S. (2023). RINGO: A RINEX pre-processing software for multi-GNSS data. Earth, Planets and Space, 75(1). https://doi.org/10.1186/s40623-023-01811-w

Kazmierski, K., Dominiak, K., & Marut, G. (2023). Positioning performance with dual-frequency low-cost GNSS receivers. Journal of Applied Geodesy. https://doi.org/10.1515/jag-2022-0042

Konakoglu, B., & Yilmaz, V. (2024). Evaluating the Performance of the Static PPP-AR in a Forest Environment. Journal of Surveying Engineering, 150(2). https://doi.org/10.1061/jsued2.sueng-1403

Krietemeyer, A., van der Marel, H., van de Giesen, N., & Ten Veldhuis, M. C. (2022). A Field Calibration Solution to Achieve High-Grade-Level Performance for Low-Cost Dual-Frequency GNSS Receiver and Antennas. Sensors, 22(6). https://doi.org/10.3390/s22062267

Romero-Andrade, R., Cabanillas-zavala, J. L., Hernández-andrade, D., Trejo-soto, M. E., & Monjardin-armenta, S. A. (2020). Análisis Comparativo Del Posicionamiento GNSS Utilizando Receptor De Bajo Costo U-Blox De Doble Frecuencia Para Aplicaciones Topógrafo-Geodésicas. European Scientific Journal, 16(27), 289–312. https://doi.org/10.19044/esj.2020.v16n27p289

Romero-Andrade, R., Trejo-Soto, M. E., Acosta-González, L. E., Hernández-Andrade, D., Nayak, K., Hernández-Columbie, V., Serrano-Agila, R., & Zambrano-Medina, Y. G. (2024). Displacements study of a dam using low-cost GNSS receivers, high precision leveling and Finite Element Model. Advances in Geodesy and Geoinformation, 55–55. https://doi.org/10.24425/agg.2024.150684

Romero-Andrade, R., Trejo-Soto, M. E., Vázquez-Ontiveros, J. R., Hernández-Andrade, D., & Cabanillas-Zavala, J. L. (2021). Sampling rate impact on Precise Point Positioning with a Low-Cost GNSS receiver. Applied Sciences (Switzerland), 11(GNSS Techniques for Land and Structure Monitoring), 17. https:// doi.org/10.3390/app11167669

Romero-Andrade, R., Zamora-Maciel, A., Uriarte-Adrián, J. D. J., Pivot, F., & Trejo-Soto, M. E. (2019). Comparative analysis of precise point positioning processing technique with GPS low-cost in different technologies with academic software. Measurement: Journal of the International Measurement Confederation, 136. https://doi.org/10.1016/j.measurement.2018.12.100

Santiago-Sánchez, L. G., Romero-Andrade, R., Trejo-Soto, M. E., Hernández-Andrade, D., Zambrano-Medina, Y. G., Alcántar-Elizondo, N., Bojorquez-Pacheco, N., Llanes-Hernández, R. M., Arana-Medina, A. I., Briseño-Morán, J. M., & Serrano-Agila, R. (2024). Análisis Comparativo del Posicionamiento Preciso Utilizando el Receptor de Bajo Costo GNSS ZED-F9P en Conjunto con la Antena BEIBT300 y Diferentes Modelos de Antena de Orden Geodésico. European Scientific Journal, 20(6), 36–55. https://doi.org/10.19044/esj.2024.v20n6p36

Sioulis, A., Tsakiri, M., & Stathas, D. (2015). Evaluation of low cost, high sensitivity GNSS receivers based on the ISO RTK standards. International Journal of Geomatics and Geosciences, 6(2), 1597–1606.

Stopar, B., Sterle, O., Pavlovčič-Prešeren, P., & Hamza, V. (2024). Observations and positioning quality of low-cost GNSS receivers: a review. GPS Solutions, 28(3), 149. https://doi.org/10.1007/s10291-024-01686-8

Takasu, T. (2013). RTKLIB 2.4.2 Manual (Number C). http://www.rtklib.com/prog/manual_2.4.2.pdf%0Ahttp://www.rtklib.com/rtklib.htm

Tsakiri, M., Sioulis, A., & Piniotis, G. (2017). Compliance of low-cost, single-frequency GNSS receivers to standards consistent with ISO for control surveying.

International Journal of Metrology and Quality Engineering, 8. https://doi.org/10.1051/ijmqe/2017006

Tunini, L., Zuliani, D., & Magrin, A. (2022). Applicability of Cost-Effective GNSS Sensors for Crustal Deformation Studies. Sensors, 22(350), 1–9. https://doi.org/ 10.3390/s22010350

Yang, J., Li, S., Zhang, A., Chen, S., & Wang, H. (2025). Performance evaluation of low-cost GNSS receivers for extracting ionospheric TEC. Astrophysics and Space Science, 370(5). https://doi.org/10.1007/s10509-025-04432-9

Zamora-Maciel, A., Romero-Andrade, R., Moraila-Valenzuela, C. R., & Pivot, F. (2020). Evaluación de receptores GPS de bajo costo de alta sensibilidad para trabajos geodésicos. Caso de estudio: línea base geodésica. Ciencia Ergo-Sum, 27, 0–17. https://doi.org/10.30878/ces.v26n2a5

Zuliani, D., Tunini, L., Severin, M., Bertoni, M., Ponton, C., & Parolai, S. (2022). LZER0: A Cost-Effective Multi-Purpose GNSS Platform. Sensors, 22(8314). https://doi.org/10.3390/s22218314

Romero-Andrade R., Alcantar-Elizondo N., Guzmán-Galindo T. D., Cañedo-Pérez J. A., Zambrano-Medina Y. G., Llanes-Hernández R. M. (2006)
Performance Evaluation of Low-Cost GNSS Receiver Using Different Geodetic Antennas in a Zero Baseline Configuration.X
Geodetski vestnik, 70 (3), 406-420.
DOI: 10.15292/geodetski-vestnik.2026.03.406-420

Ph. D. Rosendo Romero-Andrade
Faculty of Earth and Space Sciences,
Autonomous University of Sinaloa, Sinaloa, Mexico.
e-mail: r.romero11@info.uas.edu.mx

Ph. D. Norberto Alcantar-Elizondo
Faculty of Earth and Space Sciences,
Autonomous University of Sinaloa, Sinaloa, Mexico.
e-mail: noralel@uas.edu.mx

M. Sc. Tiojari D. Guzmán-Galindo
Faculty of Earth and Space Sciences,
Autonomous University of Sinaloa, Sinaloa, Mexico.
e-mail: tiohary@uas.edu.mx

B. Eng. Jorge A. Cañedo-Pérez
Faculty of Earth and Space Sciences,
Autonomous University of Sinaloa, Sinaloa, Mexico.
e-mail: jorge.canedo@uas.edu.mx

Ph. D. Yedid Gpe. Zambrano-Medina
Faculty of Earth and Space Sciences,
Autonomous University of Sinaloa, Sinaloa, Mexico.
e-mail: yedidzambrano@uas.edu.mx

B. Eng. Rafaela M. Llanes-Hernández
Faculty of Earth and Space Sciences,
Autonomous University of Sinaloa, Sinaloa, Mexico.
e-mail: rafaelallanes.facite@uas.edu.mx